

Most extremely low mass white dwarfs with non-degenerate companions are inner binaries of hierarchical triples

Felipe Lagos-Vilches,^{1*} Mercedes Hernandez,² Matthias R. Schreiber,² Steven G. Parsons,³
Boris T. Gänsicke^{1,4}

¹ *Department of physics, University of Warwick, Gibbet Hill, Coventry CV4 7AL, UK*

² *Departamento de Física, Universidad Técnica Federico Santa María, Avenida España 1680, Valparaíso, Chile*

³ *Department of Physics and Astronomy, University of Sheffield, Sheffield S3 7RH, UK*

⁴ *Centre for Exoplanets and Habitability, University of Warwick, Coventry CV4 7AL, UK*

Accepted XXX. Received YYY; in original form ZZZ

ABSTRACT

Extremely-low-mass white dwarfs (ELM WDs) with non-degenerate companions are believed to originate from solar-type main-sequence binaries undergoing stable Roche lobe overflow mass transfer when the ELM WD progenitor is at (or just past) the termination of the main-sequence. This implies that the orbital period of the binary at the onset of the first mass transfer phase must have been $\lesssim 3 - 5$ d. This prediction in turn suggests that most of these binaries should have tertiary companions since ≈ 90 per cent of solar-type main-sequence binaries in that period range are inner binaries of hierarchical triples. Until recently, only precursors of this type of binaries have been observed in the form of EL CVn binaries, which are also known for having tertiary companions. Here, we present high-angular-resolution images of TYC 6992-827-1, an ELM WD with a sub-giant (SG) companion, confirming the presence of a tertiary companion. Furthermore, we show that TYC 6992-827-1, along with its sibling TYC 8394-1331-1 (whose triple companion was detected via radial velocity variations), are in fact descendants of EL CVn binaries. Both TYC 6992-827-1 and TYC 8394-1331-1 will evolve through a common envelope phase, which depending on the ejection efficiency of the envelope, might lead to a single WD or a tight double WD binary, which would likely merge into a WD within a few Gyr due to gravitational wave emission. The former triple configuration will be reduced to a wide binary composed of a WD (the merger product) and the current tertiary companion.

Key words: binaries:close – star:evolution – white dwarfs

1 INTRODUCTION

Current theories of close white dwarf (WD) binary formation and evolution are rather limited. The most widely used prescriptions for mass transfer interactions and angular momentum loss are relatively simple conservation equations containing a number of neither theoretically nor observationally well constrained parameters (e.g., Nelemans & Tout 2005; Zorotovic et al. 2010; Ivanova et al. 2013; Belloni & Schreiber 2023). Therefore, binary population simulations are unable to reliably predict detailed characteristics of WD binary populations (Nelemans et al. 2001). Even worse, the existence of some individual systems appears to be paradoxical (e.g., Bours et al. 2015) and hundreds of WDs in wide WD+WD binaries have been found with discrepant cooling ages (Heintz et al. 2022, 2023). Consequently, observational constraints on models for the formation and evolution of close WD binaries are urgently required.

Recently, Lagos et al. (2020) showed that the occurrence rate of tertiary companions to close WD binary stars can provide information on the initial binary separation, thereby providing key insights into the

formation of the inner binary. EL CVn binaries are eclipsing systems consisting of an extremely low mass (ELM) helium WD precursor (extremely low mass is defined here as less than $0.3 M_{\odot}$) with an A/F -type main sequence companion (Maxted et al. 2014). According to Chen et al. (2017), these pre-ELM WDs with A/F main sequence companions form from solar-type close main sequence binaries with periods shorter than a few days through stable but non-conservative mass transfer. The short initial period is required to produce early mass transfer when the core of the progenitor of the pre-WD still has the low mass that we observe today in EL CVn binaries.

By observing a sample of solar-type spectroscopy binaries, Tokovinin et al. (2006) found a negative correlation between the orbital period and the frequency of tertiary companions, going from 34 to 96 per cent for orbital periods $P > 12$ and $P < 3$ days respectively (after correcting for incompleteness). This trend has been further confirmed by Laos et al. (2020) and is supported by the fact that many binaries with orbital periods of a few days or less have tertiary companions (Pribulla & Rucinski 2006; Raghavan et al. 2010; Tokovinin 2014; Hwang 2023). This correlation implies that the vast majority of EL CVn binaries should host a distant tertiary. Indeed, high contrast imaging of nearby EL CVn binaries confirmed that

* E-mail: felipe.lagos.vilches@gmail.com

Table 1. Stellar and orbital parameters for TYC 6992-827-1 reported by [Parsons et al. \(2023\)](#). ELM WD parameters were obtained from HST spectral fitting using the [Althaus et al. \(2013\)](#) cooling tracks, while sub-giant parameters were acquired through UVES spectral fitting. The orbital parameters include observations from FEROS, UVES, Du Pont, and CHIRON.

Stellar parameter	ELM WD	Sub-Giant
Mass [M_{\odot}]	0.28 ± 0.01	1.31 ± 0.14
Radius [R_{\odot}]	0.0235 ± 0.001	3.45 ± 0.12
$\log g$ [dex]	7.14 ± 0.02	3.48 ± 0.04
T_{eff} [K]	15750 ± 50	5250 ± 50
Cooling time [Myr]	6.9 ± 0.1	-
Orbital parameters		
Orbital period [d]	41.45 ± 0.01	
Semi-major axis [au]	0.27 ± 0.01	
Eccentricity	0.013 ± 0.06	

most of them are inner binaries of hierarchical triples ([Lagos et al. 2020](#)), and new EL CVn binaries with tertiary companions continue to be discovered ([Lee et al. 2024](#)).

While [Lagos et al. \(2020\)](#) only considered EL CVn binaries, ELM WDs should also form when mass transfer is initiated in a very close binary star. However, the companion stars of the large sample of ELM WDs in the ELM survey ([Brown et al. 2010](#); [Kosakowski et al. 2020](#); [Brown et al. 2020](#)) are typically WDs. This implies that two evolutionary sequences are possible. Either the ELM WD formed first, which would require stable mass transfer to occur in a close main sequence binary (such as during the formation of EL CVn binaries) and the WD companion forms in the second mass transfer phase (most likely common envelope evolution), or the first phase of mass transfer produces a short period WD plus main sequence binary and the ELM WD forms in the second (stable) mass transfer phase (e.g. [Li et al. 2023](#)).

Recently, [Parsons et al. \(2023\)](#) presented three low-mass WDs with sub-giant (SG) companion stars. These objects are perfectly consistent to have formed through dynamically stable mass transfer. The smaller the core mass of the initially more massive star at the onset of mass transfer, the shorter the initial period must have been, and the smaller is the resulting WD mass.

Two of those binaries contain ELM WDs, which implies that the period of the main-sequence binary progenitor must have been short, suggesting these systems should host distant tertiaries. Remarkably, [Parsons et al. \(2023\)](#) confirmed through radial velocity variations that one of the ELM WD+SG binaries, TYC 8394-1331-1 (hereafter TYC 8394), indeed has a tertiary companion. [Parsons et al. \(2023\)](#) therefore predicted that TYC 6992-827-1 (hereafter TYC 6992), the second ELM WD+SG binary, should also be a triple system (the stellar parameter of TYC 6992 are available in Table 1).

Here we present high-angular resolution VLT/SPHERE observations of TYC 6992 and indeed find a tertiary companion, exactly as predicted. We complement these observational results with numerical simulations of stable mass transfer using the Modules for Experiments in Stellar Astrophysics (MESA) code ([Paxton et al. 2011, 2013, 2015, 2018, 2019](#); [Jermyn et al. 2023](#)). Combining our findings with those of [Tokovinin et al. \(2006\)](#), we estimate that $\gtrsim 70$ percent of ELM WDs with non-degenerate companions should be the inner binaries of hierarchical triples.

2 OBSERVATIONS AND CHARACTERIZATION OF THE TERTIARY COMPANION

Following an observational strategy similar to that described in [Lagos et al. \(2020\)](#), we obtained high contrast images of TYC 6992 (program ID 110.243S.001) with the VLT/SPHERE instrument using the InfraRed Dual-band Imager and Spectrograph (IRDIS, [Dohlen et al. 2008](#)) in the dual band imaging mode ([Vigan et al. 2010](#)). Coronagraphic images were acquired using the $H2$ ($\lambda_{H2} = 1593$ nm) and $H3$ ($\lambda_{H3} = 1667$ nm) filter and the N-ALC-YJH-S coronagraph. The IRDIS data were pre-processed (dark background subtraction, flat-fielding, bad-pixels correction and frame recentering) with the SPHERE python package¹ version 1.6.1 ([Vigan 2020](#)).

The coronagraphic frame shown in Fig. 1 clearly reveals the presence of a tertiary candidate located at an angular separation of ≈ 117 mas from the ELM WD + SG inner binary, which corresponds to a projected separation of ≈ 59 au. For each of the 112 (7) coronagraphic (flux calibration) frames we performed aperture photometry to the tertiary candidate using an aperture of 4 pixels. This aperture is chosen to minimize the observed overlap between the tertiary and the ELM WD + SG binary (Fig. 1). Contamination coming from the quasi-azimuthal speckle patterns produced by the coronagraph at the location of the detection was estimated by calculating the flux enclosed within one aperture at the reflected location of the detection relative to the SG-WD binary. By averaging the photometry obtained for the 112 (7) coronagraphic (flux calibration) frames we derived a tertiary-to-inner binary flux ratio of 4.3 ± 0.1 and 4.1 ± 0.2 per cent in the $H2$ and $H3$ filters, respectively. Given that the WD flux is negligible in these filters relative to the SG, we can translate these flux ratios into magnitudes through synthetic photometry to the best-fit model spectrum of the SG star calculated by [Parsons et al. \(2023\)](#). By doing so, we derived $H2 \approx H3 \approx 12.72$ for the tertiary candidate.

If the tertiary is still on the main sequence, the derived magnitudes are consistent with a star of spectral type K or M, since it must have been less massive than the SG progenitor, most likely a G/late-F main-sequence star. In fact, by inspecting the isochrones for main-sequence low-mass stars of [Baraffe et al. \(2015\)](#) and assuming a current age of 9 Gyr for the entire system (≈ 7 Myr of WD cooling time from Table 1 plus 8 Gyr before the start of mass transfer according to MESA evolution tracks for a $1.1 M_{\odot}$ ELM WD progenitor), we found that the calculated $H2$ and $H3$ magnitudes are roughly consistent with a tertiary of $0.7 - 0.8 M_{\odot}$.

The probability P_{bkg} of the tertiary candidate being a false positive detection (i.e. not gravitationally bound to the ELM WD + SG binary) can be estimated by modeling as a Poisson process the occurrence of a background source down to a limiting magnitude $H_{\text{lim}} = 13$ within a radius of $\Theta = 117$ mas from the SG-WD binary. If $\rho(H_{\text{lim}})$ is the surface density of background sources down to the limiting magnitude H_{lim} , then

$$P_{\text{bkg}}(\Theta, m_{\text{lim}}) = 1 - e^{-\pi\Theta^2\rho(H_{\text{lim}})}. \quad (1)$$

To estimate $\rho(H_{\text{lim}})$, we use the Besançon galaxy model² ([Robin et al. 2004](#)) to generate a synthetic 2MASS photometric catalogue of point sources within one square degree and magnitude $H < H_{\text{lim}}$ centered on the coordinates of TYC 6992. We found that the probability of the companion to be a background source is 0.001 per

¹ <https://github.com/avigan/SPHERE>

² <https://model.obs-besancon.fr/>

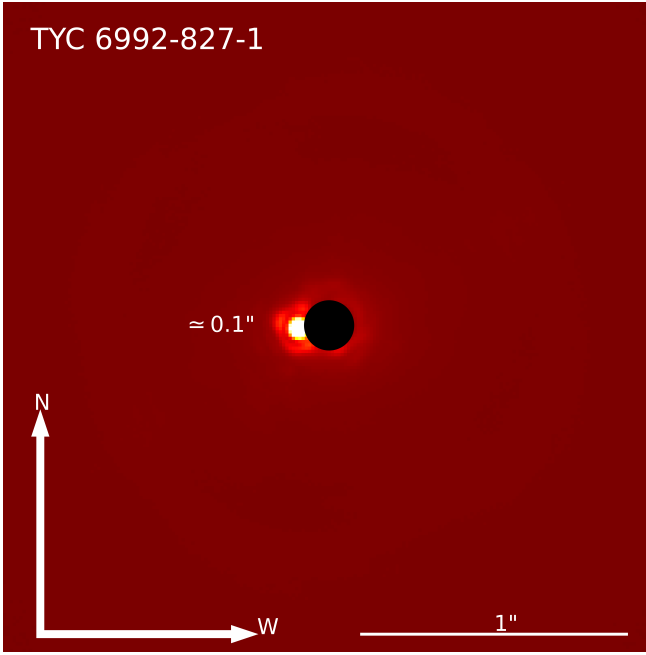


Figure 1. SPHERE/IRDIS images of TYC 6992 in the H2 band. The black circle denotes the position of the ALC_YJH_S coronagraph (RA=00:01:13.40, DEC=-33:27:06.84). The projected separation of the tertiary companion to the central binary is 117 mas corresponding to ~ 59 au at the distance of the system.

cent, suggesting that the triple candidate is most likely member of TYC 6992.

3 FORMATION SCENARIO OF ELM WD+SG BINARIES

WDs with masses $\lesssim 0.48 M_{\odot}$, such as the one observed in TYC 6992 (and TYC 8394), cannot be formed via single stellar evolution within the Hubble time. Instead, they are the product of a mass transfer event that truncates the evolution of the WD progenitor (Rebassa-Mansergas et al. 2011). Apparently single low-mass WDs likely formed through merger events (Schreiber et al. 2016; Zorotovic & Schreiber 2017).

Depending on the response of the donor star to mass loss, which depends largely on the mass ratio, mass transfer can proceed in an unstable and runaway fashion, triggering a common envelope (CE) event, or in a much more stable and self-regulated manner (see Ivanova et al. 2013; Belloni & Schreiber 2023, for recent reviews). Given its complex magneto-hydrodynamic nature, simulations of CE evolution capturing all the required details are currently unavailable. To nevertheless predict the outcome of CE evolution instead the so-called energy or α formalism is frequently used (e.g. Webbink 1984; Zorotovic et al. 2010, 2014). In this framework simple energy conservation arguments allow to estimate the final orbital period and stellar masses of a binary system at the end of the CE phase for a given value of the CE efficiency parameter. Additionally, the α formalism allows to reconstruct possible evolutionary scenarios and estimating the binary period and stellar masses at the onset of the common envelope for a given measured post-CE configuration (Nelemans & Tauris 1998; Zorotovic et al. 2010). For stable mass transfer, performing detailed simulations, e.g. with MESA, is required. Such

simulations allow to realistically track the evolution of both the stellar and orbital parameters.

In what follows, we first show that CE evolution fails at reproducing the observed properties of the ELM WD + SG binaries. We then investigate the feasibility of the stable mass transfer scenario through a set of MESA simulations.

3.1 Excluding common envelope evolution

Parsons et al. (2023) already pointed out that CE evolution is unlikely to explain the formation of both ELM WD + SG binaries characterized in their paper. We here further confirm this suggestion following the formalism proposed by Chen et al. (2017, their appendix A). In short, using the energy formalism to model the CE phase, the complete ejection of the envelope and the formation of a post-CE binary are only possible if the following criterion is satisfied:

$$\frac{0.462\alpha\lambda}{2(q_i - q_f)} \left[\frac{q_f}{q_i} \left(\frac{1 + q_i}{1 + q_f} \right)^{1/3} \left(\frac{P_i}{P_f} \right)^{2/3} - 1 \right] \left(\frac{q_i}{1 + q_i} \right)^{1/3} - 1 \geq 0. \quad (2)$$

Here q_i (q_f) is the initial (final) mass ratio M_d/M_a between the donor and the accretor star, P_i (P_f) is the orbital period at the onset (termination) of the CE phase, α the CE efficiency and λ the envelope-structure parameter (often called binding energy parameter). To obtain P_i , we assumed that the radius of the ELM WD progenitor (estimated with the radius-core mass relation for giants of Rappaport et al. (1995)) is equal to its Roche radius (estimated with the Roche lobe radius equation of Paczyński (1971)) at the onset of CE evolution. Then, by using Kepler's third law, the orbital separation at the onset of CE is translated into orbital period (Eq. A7 of Chen et al. (2017)). Since the ELM WD progenitor (the donor) must have been more massive than its companion, we have $q_i > 1$. Therefore, we explore values of q_i between 1 and 3. To ensure the most favorable scenario for a successful envelope ejection, we set $\alpha = 1$ (i.e. the orbital energy is fully converted into work in the expanding envelope) and $\lambda = 2$ (i.e. the envelope is assumed to be loosely bound to the core, as might be expected during the final stages of post-main sequence evolution (Claeys et al. 2014)).

For TYC 6992, the condition given by Eq. 2 is only met for WD masses $\gtrsim 0.56 M_{\odot}$ (see Fig. 2), far above the $0.28 M_{\odot}$ of the ELM WD. Unsurprisingly, we arrive at the same result for TYC 8394, whose ELM WD has a mass of $0.24 M_{\odot}$. Therefore, we confirm that CE evolution fails to explain their current configuration.

3.2 Evolution through stable mass transfer

We next investigated whether the stable mass transfer scenario is able to reproduce the configuration of the ELM WD + SG binaries. To that end, we used version r22.11.1 of MESA. The MESA equation of state is a blend of the OPAL (Rogers & Nayfonov 2002), SCVH (Saumon et al. 1995), FreeEOS (Irwin 2012), HELM (Timmes & Swesty 2000), PC (Potekhin & Chabrier 2010) and Skye (Jermyn et al. 2021) equations of state. Nuclear reaction rates are a combination of rates from NACRE (Angulo et al. 1999), JINA REACLIB (Cyburt et al. 2010), plus additional tabulated weak reaction rates (Fuller et al. 1985; Oda et al. 1994; Langanke & Martínez-Pinedo 2000). Screening is included via the prescription of Chugunov et al. (2007) and thermal neutrino loss rates are from Itoh et al. (1996). Electron conduction opacities are from Cassisi et al. (2007) and radiative opacities are primarily from OPAL (Iglesias & Rogers 1993,

1996), with high-temperature Compton-scattering dominated regime calculated using the equations of Buchler & Yueh (1976).

In order to ensure stable mass transfer, the initial masses of main sequence stars were chosen with consideration of the adiabatic response of the donor. This condition is typically satisfied when the initial mass ratio q_i is below a critical value known as q_{crit} . For cases involving conservative mass transfer and donors ranging between 1 and $6 M_{\odot}$, the estimated q_{crit} at the end of the red giant branch phase is approximately between 0.7 and 1 (Ge et al. 2020). The corresponding MESA simulation was initiated with a binary system on the zero-age main sequence, where the initial stellar masses are 1.1 and $0.95 M_{\odot}$, with an initial orbital period of 4.55 d. We assumed a mass loss fraction from the system during stable mass transfer of $\beta = 50$ per cent. Figure 3 illustrates the obtained formation of an extremely low mass WD through stable mass transfer.

The track shows the evolution from the moment the main-sequence ELM WD progenitor fills its Roche lobe leading to stable and non-conservative mass transfer at a rate of approximately $10^{-7} M_{\odot} \text{yr}^{-1}$. Roche-lobe overflow ends when the star reaches a radius of around $0.72 R_{\odot}$. Upon Roche lobe detachment, the pre-ELM WD is formed. This pre-ELM WD reaches its first temperature peak of around 35 000 K, which marks the start of the cooling phase. When the temperatures cooled down to ≈ 22 000 K the first hydrogen flash occurs which causes a small loop in the HR-diagram. Subsequently, the energy released during the flash results in a sharp temperature gradient near the point of maximum energy production causing the star to expand again. Following the second maximum radius, the star evolves towards high surface temperatures at a nearly constant luminosity before transitioning to the final cooling track. At an effective temperature of ≈ 30 000 K a subflash occurs which produces a similar loop as the first one but does not generate a third expansion of the star. Istrate et al. (2016) presented similar evolutionary trajectories for forming ELM WDs with neutron star companions, providing a comprehensive description of the WD’s evolution (see their section 2.2 for more details).

In Fig. 3 we also highlight the location of TYC 6992 with a cyan star symbol. The measured parameters of the ELM WD in this system are consistent with the WD having reached the final cooling track. The very similar system, TYC 8394 (its location is indicated by the cyan triangle), could represent a slightly earlier evolutionary stage just after the first hydrogen flash. Moreover, the 14 WD progenitors with stripped low-mass giants (yellow dots) documented by El-Badry & Rix (2022) are accurately reproduced by our track during the initial stable (non-conservative) mass transfer phase. The five EL CVn with tertiary companions reported by Lagos et al. (2020) represent a later evolutionary stage which is reached after mass transfer ended and hydrogen flashes cause the star to expand again. We thus conclude that parameters of ELM WDs with non-degenerate companions, such as those characterized by Parsons et al. (2023), are consistent with having formed through stable mass transfer.

3.3 The effect of triple dynamics prior and after the mass transfer phase

Inner binaries in triple systems can undergo orbital shrinkage due to the combined effect of high eccentricity incursions induced by the tertiary companion through the Von Zeipel-Lidov-Kozai (ZLK) mechanism and tidal friction at (or near) periastron (aka Kozai cycles with tidal friction or KCTF, Fabrycky & Tremaine 2007; Shappee & Thompson 2013; Naoz & Fabrycky 2014).

To estimate whether the the main sequence binary progenitor assumed in section 3.2 could have experienced KCTF, we simulate

the evolution of a triple systems composed of an inner circular binary with stellar masses 1.1 and $0.95 M_{\odot}$, with its semi-major axis ranging from 0.1 to 1.1 au in steps of 0.2 au, outer binary with eccentricity 0.5, semi-major axis of 10 au and tertiary mass of $0.8 M_{\odot}$. The mutual inclination between the inner and outer orbits is set to 70 degrees. The choice of mutual inclination and outer eccentricity values, though somewhat arbitrary, favors the occurrence of high eccentricity incursions while remaining within the observed range derived by Borkovits et al. (2015, 2016) and Czavalinga et al. (2023), where higher values are less common. Similarly, the outer semi-major axis is chosen to enhance the ZLK mechanism while maintaining the secular dynamical stability of the system.

We use the MULTIPLE STELLAR EVOLUTION³ (MSE, Hamers et al. 2021) code (version 0.87) to calculate the secular orbital evolution of the inner binary, including the effects of stellar and tidal evolution, general relativity, N-body dynamics and binary interactions. In all our simulations, we found that while the ZLK mechanism can induce inner eccentricities as high as $\approx 0.8 - 0.9$ during the main sequence, the tidal forces are not strong enough to cause significant inward migration. Only once the $1.1 M_{\odot}$ star reaches the red giant phase does the inner orbit start to shrink. At this stage, however, the core mass exceeds $0.28 M_{\odot}$ (i.e. the mass of the observed ELM WD), which fails to explain the current configuration of TYC 6992. Although we cannot rule out the possibility that a different initial orbital configuration might produce more extreme eccentricity incursions (enhancing the effect of tides at periastron), such a scenario would require higher and less likely values for the outer eccentricity and mutual inclination. This, in turn, might require an initial outer semi-major axis greater than 10 au to ensure the secular stability of the system, which would also weaken the ZLK mechanism. We emphasize that although this analysis is based on a set of initial conditions favouring the occurrence of high eccentricity incursions, a full exploration of the orbital parameter space—beyond the scope of this paper—is needed to properly assess the role of triple dynamics in TYC 6992.

It is important to note that, whether the inner binary was born with a short orbital period or underwent migration via KCTF, does not change the fact that the currently observed parameters of TYC 6992 are fully consistent with a formation through stable mass transfer. The main aim of this paper is to explore the relation between ELM WDs with close non-degenerate companions and the existence of tertiaries. Whether triple dynamics played a role in the formation of the short period of the inner binary prior to mass transfer is of minor importance here. However, we note that the observed relation between the period of main sequence binaries and the existence of a tertiary (Tokovinin et al. 2006) cannot be fully explained by triple dynamics (Borkovits et al. 2015, 2016; Moe & Kratter 2018).

In its current configuration, assuming an outer semi-major axis of 60 au and an eccentricity of 0.5, the ZLK eccentricity oscillation timescale is ≈ 800 Myr (using Eq. 41 of Antognini 2015, with $m_2 \neq 0$). As discussed in Parsons et al. (2023), this system is expected to undergo a common envelope phase in $\sim 200 - 300$ Myr, making it very unlikely that triple dynamics have any significant impact on the future evolution of TYC 6992.

³ <https://github.com/hamers/mse>

4 PREDICTING THE TRIPLE FRACTION

Having confirmed that observed ELM WDs with non-degenerate companions must form through stable mass transfer, we now use the statistics of tertiary companions to close main sequence binaries (Tokovinin et al. 2006) to estimate the fraction of such binaries that should host a distant tertiary. To that end, we performed a series of 58 MESA simulations for a zero-age-main-sequence binary with primary and secondary star masses of 1.1 and 0.95 M_{\odot} , respectively. Again, the simulations incorporate a mass loss fraction from the system of $\beta = 50$ per cent during stable mass transfer. The initial orbital period was varied from 1 to 30 d.

In Fig. 4, we present the relation between the helium core mass (i.e. the ELM WD mass) obtained from the evolution of the primary component of the binary as a function of its initial orbital period. As expected, longer initial periods produce more massive WDs as the primary is able to evolve in isolation for a longer period of time before filling its Roche lobe. For an initial period of ≈ 4.5 d, the resulting final orbital period and ELM WD mass are in agreement with those values of TYC 6992. As is well known, a relatively tight relation exists between the final period and the WD mass of post-stable mass transfer binaries (e.g. Parsons et al. 2023). The period of TYC 8394 (51.8 d) is only slightly longer than TYC 6992 (41.5 d) and the WD mass is also very similar (0.24 and 0.28 M_{\odot} for TYC 8394 and TYC 6992, respectively), so that a perfect match for TYC 8394 could certainly be obtained by varying the initial masses.

We compare the resulting relationship between initial period and WD mass with the frequency of tertiary companions as a function of the initial orbital period of a close main sequence binary from Tokovinin et al. (2006). In all cases where binaries have an initial orbital period below six days, they eventually form a WD with a mass of up to 0.29 M_{\odot} . These binaries have a probability exceeding 70 percent of hosting a tertiary companion consistent with our observations.

For completeness we note that, as we fixed the initial masses, the relation between initial period and WD mass shown in Fig. 4 does not reflect the full set of possible solutions. However, for slightly different initial masses, that is, for binaries with initial masses similar to the Sun ($\sim 0.8\text{--}1.3 M_{\odot}$), the relation between initial period and resulting WD mass will change only slightly, as the Roche-volume of the more massive star will also change only slightly. Therefore, our conclusion for the occurrence of tertiaries remains true as long as the initial masses are similar to that of the Sun. ELM WDs can also form from close binaries consisting of significantly more massive stars. In this case the non-degenerate star must be more massive as well and the triple statistic from Tokovinin et al. (2006) no longer applies.

5 THE FUTURE OF TYC 6992-827-1

The detached phase of TYC 6992, which might include a short symbiotic phase (Parsons et al. 2023), will continue until the SG star fills its Roche lobe, starting a second mass transfer episode. Since the mass ratio of the binary is well above the critical mass ratio ($q_{\text{crit}} \approx 0.7\text{--}1$), mass transfer will proceed unstably, triggering a CE phase. If the envelope is ejected, then the orbital semi-major axis of the resulting double WD binary is given by

$$a_f = \frac{M_{\text{SG,core}} M_{\text{ELM}}}{2M_{\text{SG}} \left(\frac{M_{\text{ELM}}}{2a_i} - \frac{M_{\text{SG,env}}}{\lambda \alpha R_{\text{SG}}} \right)}, \quad (3)$$

where $M_{\text{SG,core}}$, $M_{\text{SG,env}}$ and M_{SG} are the core, envelope and

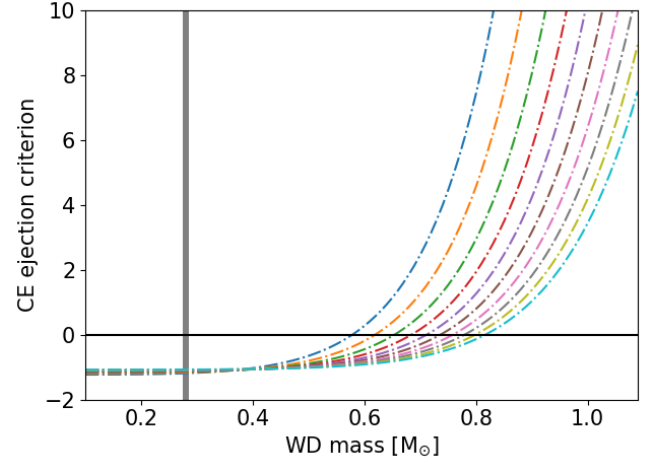


Figure 2. CE ejection criterion (left side of Equation 2) using $\alpha = 1$ and $\lambda = 2$ as function of the WD mass for TYC 6992. Dash-dotted lines consider initial mass ratios from 1 (blue) to 3 (cyan) in steps of 0.2. For the observed orbital configuration of TYC 6992 CE evolution is only possible for WD masses $\geq 0.56 M_{\odot}$ (i.e. above the black line at $y = 0$). Therefore, a WD with $0.28 \pm 0.01 M_{\odot}$ (gray area) like the one in TYC 6992 could not have formed via CE evolution.

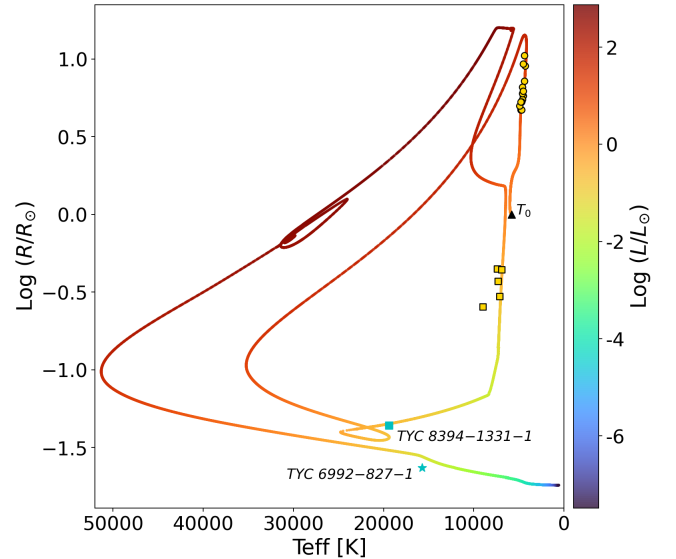


Figure 3. Radius evolution plotted against the effective temperature of a main-sequence binary with initial stellar masses of 1.1 and 0.95 M_{\odot} and an initial orbital period of 4.55 d (T_0 is indicated with the black arrow which also show the direction of the evolution), evolved in MESA. The color code of the line corresponds to the luminosity evolution of the 1.1 M_{\odot} WD progenitor. Yellow dots and squares represent the WD progenitors from El-Badry & Rix (2022) and ELCVns from Lagos et al. (2020) respectively, while the blue star represent TYC 6992. The blue square show the spot that correspond to the similar binary TYC 8394 from Parsons et al. (2023).

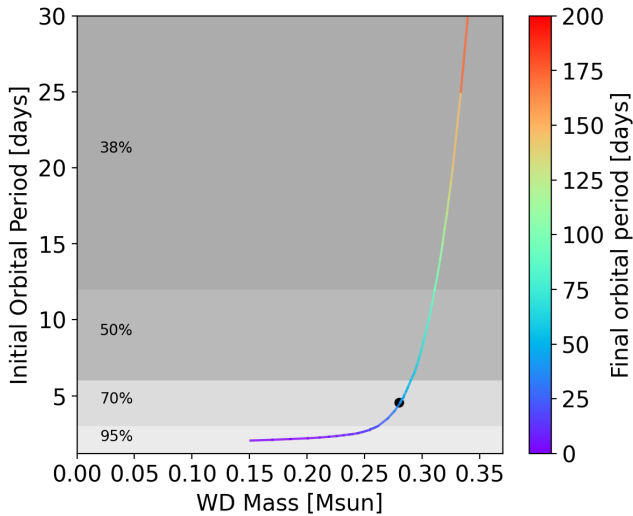


Figure 4. The mass of the helium core formed during the MESA evolution of a main-sequence star with a mass of $1.1 M_{\odot}$ is expressed in terms of the initial orbital period of the binary system. The black dot corresponds to observations of TYC 6992-827-1, while the color code of the line corresponds to the final orbital period of each binary simulated with MESA. The grey shaded areas indicate the boundaries of the initial orbital period and the corresponding probability of the system having a tertiary companion (taken from Fig. 14 of Tokovinin et al. 2006).

total mass of the SG star, respectively, R_{SG} the radius of the SG star at the onset of CE, M_{ELM} the mass of the ELM WD, and a_i the semi-major axis at the onset of the CE phase. By taking a referential $1.3 M_{\odot}$ evolutionary track from the MESA Isochrones and Stellar Tracks (MIST, Paxton et al. 2011; Dotter 2016; Choi et al. 2016), we have $M_{\text{SG,core}} = 0.32 M_{\odot}$, $M_{\text{SG,env}} = 0.97 M_{\odot}$ and $R_{\text{SG}} = 30 R_{\odot}$. For envelope-structure values consistent with sub-giant stars ($\lambda \approx 0.25 - 0.75$ Claeys et al. 2014), two outcomes are possible depending on the common envelope ejection efficiency (Fig. 5): if $\alpha \gtrsim 0.25$, the envelope is ejected and the resulting double WD would have an orbital period between 3 min and 3.6 h (similar to the population of tight WD+WD binaries predicted by Shariat et al. (2023), their figure 6). At such orbital periods, angular momentum loss due to gravitational radiation becomes important, leading to the merger of the two WDs on timescales ranging from approximately 0.3 Myr to a few Gyr (Brown et al. 2016). On the other hand, if $\alpha \lesssim 0.25$, the binary is prone to a merger event, likely ending up as a single WD somewhat more massive than the current ELM WD, as suggested by Parsons et al. (2023). This scenario is consistent with the merging population of ELM WD + red giant binaries with orbital periods > 10 d predicted by Shariat et al. (2024, their Fig. 6).

In both outcomes, the resulting wide binary composed of a WD and a K/M-type companion (the current tertiary) will resemble the configuration of HE 0430—2457, the first ELM WD found in a wide binary with a K-type companion, whose origin is also attributed to the merger of an inner binary in a hierarchical triple (Vos et al. 2018). Given its similarity to TYC 6992, both scenarios, the survival of a close binary inner binary or the merger of the inner binary, also apply to TYC 8394.

6 DISCUSSION

We have shown that the current configuration of the two ELM WD + SG binaries discovered by Parsons et al. (2023) can only be explained if the former main-sequence binary has an orbital period $\lesssim 5$ d and passes through a phase of stable mass transfer when the ELM WD progenitor is at the end of (or just leaving) the main-sequence. The discovery of tertiary companions around these systems, either by direct imaging or radial velocity monitoring, provides further support to this formation channel and highlights their similarities to EL CVn-type binaries. Given that the main difference between both type of binaries is the evolutionary stage of the stellar components, ELM WD + SG binaries are most likely descendants of EL CVn binaries.

The past history of EL CVn-like binaries has recently been unveiled by El-Badry & Rix (2022). They discovered 14 binaries composed of a highly stripped low-mass giant (the future ELM WD) and a $\approx 2 M_{\odot}$ main-sequence companion. Using MESA simulations they found evolution tracks similar to those derived by Chen et al. (2017) for EL CVn binaries. Additionally, they identified similar main-sequence binary progenitors: low-mass giant progenitors with $\approx 1 M_{\odot}$, initial mass ratios $0.6 \lesssim q_i \lesssim 0.9$ and orbital periods of ≈ 1 d (see figure 4 of Chen et al. 2017). This sample of pre-EL CVn binaries also perfectly aligns with the stellar radius-effective temperature evolutionary track of our canonical binary setup shown in Fig. 3. Hence, it is reasonable to expect that these pre-EL CVn systems should also have tertiary companions. In an attempt to look for them, we cross-match the sample of pre-EL CVn binaries with the Gaia-based catalog of resolved binaries of El-Badry et al. (2021) and find that the closest (≈ 720 pc) pre-EL CVn system (Gaia DR3 5243109471519822720) has in fact a wide companion (Gaia DR3 5243109471512749056) with a projected separation of ≈ 2375 au. Since the remaining 13 systems have distances $\gtrsim 900$ pc, the identification of additional companions is severely hindered by the angular resolution (and sensitivity) of Gaia. To improve the likelihood of detection, high-angular resolution and high-contrast imaging are required (e.g. Lagos et al. 2020).

It is worth noting that Garbutt et al. (2024) and Shahaf et al. (2024) identified a sample of WDs with main sequence companions of spectral type F, G, K with long periods (exceeding several hundred days) that are not consistent with the predictions of stable mass transfer (see their figure 8). Systems with WD masses exceeding $0.6 M_{\odot}$ are most likely post common envelope binaries that started mass transfer when the WD progenitor was on the late asymptotic giant branch (Belloni et al. 2024a,b). However, those binaries with orbital periods of hundreds of days but containing ELM WDs cannot have formed through common envelope evolution and, according to the orbital period-WD mass relation shown in the upper panel of Fig. 8 in Garbutt et al. (2024), are also difficult to explain through stable mass transfer. A dedicated survey for tertiaries to these close binaries could provide evidence for their formation through stable mass transfer. If the existence of tertiaries can be confirmed at a high rate ($\gtrsim 70$ per cent), a currently unknown mechanism producing wider orbits than predicted by standard models of stable mass transfer must be at work.

A similar puzzling situation has been claimed to exist for the self-lensing binary KIC 8145411, initially identified as a $0.2 M_{\odot}$ ELM WD with an orbital period of 456 d around a solar-type companion (Masuda et al. 2019). However, Yamaguchi et al. (2024) discovered an additional unresolved tertiary companion that altered the mass estimation, revealing that the WD mass is larger than previously thought ($0.53 M_{\odot}$) and consistent with CE evolution. In principle, the presence of additional unresolved companions to the astrometric

ELM WD + MS binaries could similarly alter the estimation of the corresponding WD masses. However, again, this potential solution remains speculative unless more unresolved tertiaries are discovered.

The fact that most ELM WD with non-degenerate companions are inner binaries of hierarchical triples raises the question of whether triple dynamics is primarily responsible for their formation by triggering the inward orbital migration necessary for stable mass transfer. While Fabrycky & Tremaine (2007) showed that KCTF is able to produce close ($P < 10$ d) binaries, Moe & Kratter (2018) found that KCTF is only able to produce ≈ 40 per cent of such binaries. The remaining 60 per cent are most likely formed due to disc fragmentation followed by inward migration caused by energy dissipation from interactions with the primordial gas during the pre-main-sequence. As discussed by Lagos et al. (2020), the presence of tertiary companions around EL CVn binaries might be a fingerprint of the initial formation conditions. Either the initial mass required for migration to work is large enough that it is virtually always accompanied by the formation of a tertiary via core fragmentation or the tertiary is triggering disc fragmentation at an early stage when there is still enough gas for migration to take place.

For the five EL CVn binaries found by Lagos et al. (2020) and the pre-EL CVn in the El-Badry et al. (2021) catalogue, we find that the ZLK oscillation timescale is on the order of several Gyr in most cases, supporting the pre-main-sequence migration scenario. This estimate is derived by using half of the projected separation of the tertiary (to account for potential orbital widening due to mass loss) as a proxy of the outer semi-major axis, while assuming an outer eccentricity of 0.7, inner period of five days and nominal stellar masses for EL CVn systems (i.e. a $1M_{\odot}$ twin inner binary and $0.8M_{\odot}$ tertiary). The pre-main-sequence migration scenario is also consistent with the twin and close nature of the EL CVn progenitor binaries. As discussed by Tokovinin (2000), the population of twin solar-type close binaries can be explained by primordial circumbinary discs massive enough to simultaneously enable accretion and inward migration, while also enhancing the possibility of capturing a tertiary companion by dissipating its gravitational energy.

While the smaller projected separations of the tertiary companion in TYC 6992 and the highly compact nature of TYC 8394 (with an outer semi-major axis of ≈ 2.2 au) suggests that KCTF could have played a role in the formation of the triple configuration prior to mass transfer, this scenario is somewhat disfavored by the fact that triple systems with outer projected separations $\lesssim 50$ au tend to have coplanar orbits (Tokovinin 2017). The discovery and characterization of additional close tertiary companions around ELM WDs with non-degenerate companions could offer further insights into their formation mechanism(s).

7 CONCLUSIONS

We report the discovery, through direct imaging, of a tertiary companion around the binary TYC 6992-827-1, consisting of a sub-giant star and a ELM WD. By reconstructing its evolutionary history, we found that it follows the same evolutionary path as EL CVn binaries, which are composed of a pre-ELM WD and a main-sequence companion of spectral type A/F. Our binary evolution simulations also naturally reproduce the observed stellar radius-effective temperature relation of the ELM WD progenitor star in pre-EL CVn binaries. Therefore, TYC 6992-827-1 (and its sibling TYC 8394-1331-1) represent an later evolutionary stage of EL CVn binaries in which the companion to the ELM WD just left the main sequence. This is consistent with the triple nature of TYC 6992-827-1 and TYC 8394-1331-1 and most

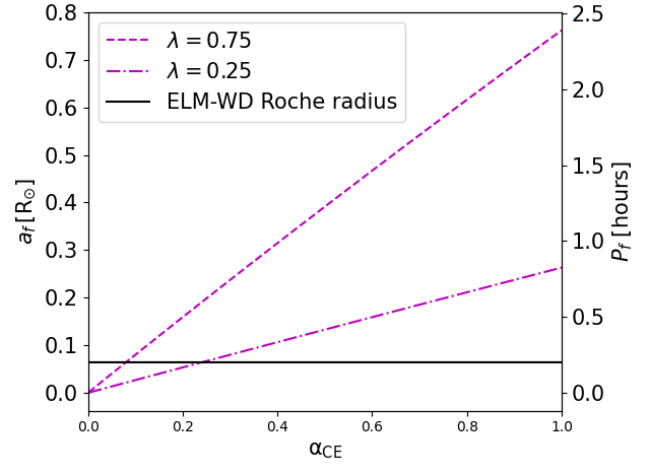


Figure 5. Final orbital semi-major axis (or its equivalent orbital period P_f) of the post CE double WD TYC 6992 as function of the common envelope efficiency parameter α for two limiting values of λ . The solid black line represents the minimum semi-major axis before the ELM WD fills its Roche lobe. For highly efficient envelope ejections (i.e. $\alpha \approx 1$) the value of a_f (P_f) ranges from 0.26 (0.82) to 0.76 (2.4) R_{\odot} (h), while for less efficient ejections ($0.08 \lesssim \alpha \lesssim 0.25$) the minimum value for a_f (P_f) is $\approx 0.06R_{\odot}$ (≈ 0.2 h).

EL CVn binaries (Lagos et al. 2020) which indicates that all these systems form from short period main sequence binary stars. EL CVn binaries and their late evolutionary stage in the form of ELM WD + sub-giant binaries are currently the only known examples where an ELM WD has a non-degenerate companion.

We estimate that TYC 6992-827-1 (and also TYC 8394-1331-1) will experience a common envelope phase in the future. Depending on how efficient orbital energy is used to expel the envelope, the final product could be either a single WD or a tight double WD binary which would merge into a single WD within a few Gyr. Thus, the former triples system will become wide binaries composed of a WD and a K-type main-sequence companion.

ACKNOWLEDGEMENTS

We thank the anonymous referee for their helpful comments and suggestions. This project has received funding from the European Research Council (ERC) under the European Union’s Horizon 2020 Research and Innovation Programme (grant agreement no. 101020057). MRS thanks for support from FONDECYT (grant number 1221059). Based on observations collected at the European Southern Observatory under ESO programme 110.243S.001.

DATA AVAILABILITY

The data and numerical tools used in this article can be obtained upon request to the corresponding author and after agreeing to the terms of use.

REFERENCES

- Althaus L. G., Miller Bertolami M. M., Córscico A. H., 2013, *A&A*, **557**, A19
 Angulo C., et al., 1999, *Nuclear Phys. A*, **656**, 3
 Antognini J. M. O., 2015, *MNRAS*, **452**, 3610

- Baraffe I., Homeier D., Allard F., Chabrier G., 2015, *A&A*, **577**, A42
- Belloni D., Schreiber M. R., 2023, in , *Handbook of X-ray and Gamma-ray Astrophysics*. Edited by Cosimo Bambi and Andrea Santangelo. p. 129, doi:10.1007/978-981-16-4544-0_98-1
- Belloni D., Zorotovic M., Schreiber M. R., Parsons S. G., Moe M., Garbutt J. A., 2024a, *arXiv e-prints*, p. arXiv:2401.07692
- Belloni D., Schreiber M. R., Zorotovic M., 2024b, *arXiv e-prints*, p. arXiv:2401.17510
- Borkovits T., Rappaport S., Hajdu T., Sztakovics J., 2015, *MNRAS*, **448**, 946
- Borkovits T., Hajdu T., Sztakovics J., Rappaport S., Levine A., Bíró I. B., Klagyivik P., 2016, *MNRAS*, **455**, 4136
- Bours M. C. P., et al., 2015, *MNRAS*, **450**, 3966
- Brown W. R., Kilic M., Prieto C. A., Kenyon S. J., 2010, *The Astrophysical Journal*, **723**, 1072–1081
- Brown W. R., Kilic M., Kenyon S. J., Gianninas A., 2016, *ApJ*, **824**, 46
- Brown W. R., et al., 2020, *ApJ*, **889**, 49
- Buchler J. R., Yueh W. R., 1976, *ApJ*, **210**, 440
- Cassisi S., Potekhin A. Y., Pietrinferni A., Catelan M., Salaris M., 2007, *ApJ*, **661**, 1094
- Chen X., Maxted P. F. L., Li J., Han Z., 2017, *MNRAS*, **467**, 1874
- Choi J., Dotter A., Conroy C., Cantiello M., Paxton B., Johnson B. D., 2016, *ApJ*, **823**, 102
- Chugunov A. I., Dewitt H. E., Yakovlev D. G., 2007, *Phys. Rev. D*, **76**, 025028
- Claeys J. S. W., Pols O. R., Izzard R. G., Vink J., Verbunt F. W. M., 2014, *A&A*, **563**, A83
- Cybur R. H., et al., 2010, *ApJS*, **189**, 240
- Czavalinga D. R., Mitnyan T., Rappaport S. A., Borkovits T., Gagliano R., Omohundro M., Kristiansen M. H. K., Pál A., 2023, *A&A*, **670**, A75
- Dohlen K., et al., 2008, The infra-red dual imaging and spectrograph for SPHERE: design and performance. SPIE, p. 70143L, doi:10.1117/12.789786
- Dotter A., 2016, *ApJS*, **222**, 8
- El-Badry K., Rix H.-W., 2022, *MNRAS*, **515**, 1266
- El-Badry K., Rix H.-W., Heintz T. M., 2021, *MNRAS*, **506**, 2269
- Fabrycky D., Tremaine S., 2007, *ApJ*, **669**, 1298
- Fuller G. M., Fowler W. A., Newman M. J., 1985, *ApJ*, **293**, 1
- Garbutt J. A., et al., 2024, *MNRAS*, **529**, 4840
- Ge H., Webbink R. F., Chen X., Han Z., 2020, *ApJ*, **899**, 132
- Hamers A. S., Rantala A., Neunteufel P., Preece H., Vynatheya P., 2021, *MNRAS*, **502**, 4479
- Heintz T. M., Hermes J. J., El-Badry K., Walsh C., van Saders J. L., Fields C. E., Koester D., 2022, *ApJ*, **934**, 148
- Heintz T. M., Hermes J. J., El-Badry K., Walsh C., van Saders J. L., Fields C. E., Koester D., 2023, *ApJ*, **952**, 92
- Hwang H.-C., 2023, *MNRAS*, **518**, 1750
- Iglesias C. A., Rogers F. J., 1993, *ApJ*, **412**, 752
- Iglesias C. A., Rogers F. J., 1996, *ApJ*, **464**, 943
- Irwin A. W., 2012, FreeEOS: Equation of State for stellar interiors calculations, Astrophysics Source Code Library, record ascl:1211.002
- Istrate A. G., Marchant P., Tauris T. M., Langer N., Stancliffe R. J., Grassitelli L., 2016, *A&A*, **595**, A35
- Itoh N., Hayashi H., Nishikawa A., Kohyama Y., 1996, *ApJS*, **102**, 411
- Ivanova N., et al., 2013, *A&ARv*, **21**, 59
- Jermyn A. S., Schwab J., Bauer E., Timmes F. X., Potekhin A. Y., 2021, *ApJ*, **913**, 72
- Jermyn A. S., et al., 2023, *ApJS*, **265**, 15
- Kosakowski A., Kilic M., Brown W. R., Gianninas A., 2020, *ApJ*, **894**, 53
- Lagos F., Schreiber M. R., Parsons S. G., Gänsicke B. T., Godoy N., 2020, *MNRAS*, **499**, L121
- Langanke K., Martínez-Pinedo G., 2000, *Nuclear Phys. A*, **673**, 481
- Laos S., Stassun K. G., Mathieu R. D., 2020, *ApJ*, **902**, 107
- Lee J. W., Hong K., Jeong M.-J., Wolf M., 2024, *arXiv e-prints*, p. arXiv:2407.17729
- Li Z., Chen X., Ge H., Chen H.-L., Han Z., 2023, *A&A*, **669**, A82
- Masuda K., Kawahara H., Latham D. W., Bieryla A., Kunitomo M., MacLeod M., Aoki W., 2019, *ApJ*, **881**, L3
- Maxted P. F. L., et al., 2014, *MNRAS*, **437**, 1681
- Moe M., Kratter K. M., 2018, *ApJ*, **854**, 44
- Naoz S., Fabrycky D. C., 2014, *ApJ*, **793**, 137
- Nelemans G., Tauris T. M., 1998, *A&A*, **335**, L85
- Nelemans G., Tout C. A., 2005, *MNRAS*, **356**, 753
- Nelemans G., Yungelson L. R., Portegies Zwart S. F., Verbunt F., 2001, *A&A*, **365**, 491
- Oda T., Hino M., Muto K., Takahara M., Sato K., 1994, *Atomic Data and Nuclear Data Tables*, **56**, 231
- Paczynski B., 1971, *ARA&A*, **9**, 183
- Parsons S. G., et al., 2023, *MNRAS*, **518**, 4579
- Paxton B., Bildsten L., Dotter A., Herwig F., Lesaffre P., Timmes F., 2011, *ApJS*, **192**, 3
- Paxton B., et al., 2013, *ApJS*, **208**, 4
- Paxton B., et al., 2015, *ApJS*, **220**, 15
- Paxton B., et al., 2018, *ApJS*, **234**, 34
- Paxton B., et al., 2019, *ApJS*, **243**, 10
- Potekhin A. Y., Chabrier G., 2010, *Contributions to Plasma Physics*, **50**, 82
- Pribulla T., Rucinski S. M., 2006, *AJ*, **131**, 2986
- Raghavan D., et al., 2010, *ApJS*, **190**, 1
- Rappaport S., Podsiadlowski P., Joss P. C., Di Stefano R., Han Z., 1995, *MNRAS*, **273**, 731
- Rebassa-Mansergas A., Nebot Gómez-Morán A., Schreiber M. R., Girven J., Gänsicke B. T., 2011, *MNRAS*, **413**, 1121
- Robin A. C., Reylé C., Derrière S., Picaud S., 2004, *A&A*, **416**, 157
- Rogers F. J., Nayfonov A., 2002, *ApJ*, **576**, 1064
- Saumon D., Chabrier G., van Horn H. M., 1995, *ApJS*, **99**, 713
- Schreiber M. R., Zorotovic M., Wijnen T. P. G., 2016, *MNRAS*, **455**, L16
- Shahaf S., Hallakoun N., Mazeh T., Ben-Ami S., Rekhi P., El-Badry K., Toonen S., 2024, *MNRAS*, **529**, 3729
- Shappee B. J., Thompson T. A., 2013, *ApJ*, **766**, 64
- Shariat C., Naoz S., Hansen B. M. S., Angelo I., Michaely E., Stephan A. P., 2023, *ApJ*, **955**, L14
- Shariat C., Naoz S., El-Badry K., Rodriguez A. C., Hansen B. M. S., Angelo I., Stephan A. P., 2024, *arXiv e-prints*, p. arXiv:2407.06257
- Timmes F. X., Swesty F. D., 2000, *ApJS*, **126**, 501
- Tokovinin A. A., 2000, *A&A*, **360**, 997
- Tokovinin A., 2014, *AJ*, **147**, 87
- Tokovinin A., 2017, *ApJ*, **844**, 103
- Tokovinin A., Thomas S., Sterzik M., Udry S., 2006, *A&A*, **450**, 681
- Vigan A., 2020, vlt-sphere: Automatic VLT/SPHERE data reduction and analysis (ascl:2009.002), doi:10.5281/zenodo.6563998
- Vigan A., Moutou C., Langlois M., Allard F., Boccaletti A., Carbillet M., Mouillet D., Smith I., 2010, *MNRAS*, **407**, 71
- Vos J., Zorotovic M., Vučković M., Schreiber M. R., Østensen R., 2018, *MNRAS*, **477**, L40
- Webbink R. F., 1984, *ApJ*, **277**, 355
- Yamaguchi N., El-Badry K., Ciardi D. R., Latham D. W., Masuda K., Bieryla A., Clark C. A., Condon S. S., 2024, *arXiv e-prints*, p. arXiv:2405.00780
- Zorotovic M., Schreiber M. R., 2017, *MNRAS*, **466**, L63
- Zorotovic M., Schreiber M. R., Gänsicke B. T., Nebot Gómez-Morán A., 2010, *A&A*, **520**, A86
- Zorotovic M., Schreiber M. R., García-Berro E., Camacho J., Torres S., Rebassa-Mansergas A., Gänsicke B. T., 2014, *A&A*, **568**, A68

This paper has been typeset from a $\text{\TeX}/\text{\LaTeX}$ file prepared by the author.